The ciliary protein IFT88 controls post-natal cartilage thickness and influences development of osteoarthritis.

Coveney CR[1], Zhu L[1], Miotla-Zarebska J[1], Stott B[1], Parisi I[1], Batchelor V[1], Duarte C[1], Chang E[1], McSorley E[1], Vincent TL[1], Wann AKT[1]

[1]Kennedy Institute of Rheumatology, University of Oxford, Oxford, United Kingdom

Correspondence to:
*Clarissa R Coveney, DPhil (Oxon)
Kennedy Institute of Rheumatology
University of Oxford
Roosevelt Drive
Oxford
OX3 7FY
Email: clarissa.coveney@kennedy.ox.ac.uk

Conflict of interest

TLV ad hoc consultancy in past 2 years for Mundipharma and GSK

Keywords: Cartilage thickness, Atrophy, Primary cilium, IFT88, Calcification

Abstract

Mechanical forces are known to drive cellular signalling programmes in cartilage development, health, and disease. Proteins of the primary cilium, implicated in mechanoregulation, control cartilage formation during skeletal development, but their role in post-natal cartilage is unknown. *Ift88*$^{fl/fl}$ and *AggrecanCreER*^{T2} mice were crossed to create a cartilage specific inducible knockout mouse *AggrecanCreER*^{T2}*;Ift88*$^{fl/fl}$. Tibial articular cartilage thickness was assessed, through adolescence and adulthood, by histomorphometry and integrity by OARSI score. *In situ* cell biology was investigated by immunohistochemistry (IHC) and qPCR of micro-dissected cartilage. OA was induced by destabilisation of the medial meniscus (DMM). Some mice were provided with exercise wheels in their cage. Deletion of IFT88 resulted in a reduction in medial articular cartilage thickness (atrophy) during adolescence from 102.57µm, 95% CI [94.30, 119.80] in control (*Ift88*$^{fl/fl}$) to 87.36µm 95% CI [81.35, 90.97] in *AggrecanCreER*^{T2}*;Ift88*$^{fl/fl}$ by 8-weeks $p<0.01$, and adulthood (104.00µm, 95% CI [100.30, 110.50] in *Ift88*$^{fl/fl}$ to 89.42µm 95% CI [84.00, 93.49] in *AggrecanCreER*^{T2}*;Ift88*$^{fl/fl}$, 34-weeks, $p<0.0001$) through a reduction in calcified cartilage. Thinning in adulthood was associated with spontaneous cartilage degradation. Following DMM, *AggrecanCreER*^{T2}*;Ift88*$^{fl/fl}$ mice had increased OA (OARSI scores at 12 weeks *Ift88*$^{fl/fl}$ = 22.08 +/- 9.30, and *AggrecanCreER*^{T2}*;Ift88*$^{fl/fl}$ = 29.83 +/- 7.69). Atrophy was not associated with aggrecanase-mediated destruction or chondrocyte hypertrophy. *Ift88* expression positively correlated with *Tcf7l2* and connective tissue growth factor. Cartilage thickness was restored in *AggrecanCreER*^{T2}*;Ift88*$^{fl/fl}$ by voluntary wheel exercise. Our results demonstrate that ciliary IFT88 regulates cartilage thickness and is chondroprotective, potentially through modulating mechanotransduction pathways in articular chondrocytes.

Introduction

The key function of articular cartilage is to absorb and transmit mechanical loads generated by muscle contraction and weight-bearing during physical activity. This is achieved by having an intact articular surface and by the tissue being able to mechanoadapt its structure according to a change in the mechanical environment. Cartilage can be broadly divided into a non-calcified and a calcified zone adjacent to bone; its total thickness is allometrically scaled to the organism size ensuring chondrocytes experience similar force irrespective of animal mass [1]. Articular cartilage is extremely mechanosensitive, with chondrocytes closely monitoring and remodelling the extracellular matrix in response to physiological loads [2, 3]. Physiological mechanical loading has long been established to be critical for cartilage development and homeostasis [4]. Loss of mechanical load leads to thinning (atrophy) of cartilage [5, 6]. Pathological, supraphysiological mechanical loading predisposes to the development of osteoarthritis (OA), where degradation of the cartilage occurs with loss of integrity of the articular surface [6].

The cellular response to mechanical force includes the release of fibroblast growth factor 2 (FGF2), transforming growth factor beta (TGFβ) from the matrix upon mechanical load, and activation of Hedgehog (Hh) ligand, indian hedgehog (IHH) [7-10]. A number of other pathways are implicated in cellular mechanotransduction including connexin and ion channel opening and integrin activation. How chondrocytes integrate these cues as cartilage matures through adolescence, adapting to prepare for life-long loading, is not completely understood.

Along with most cells of the body articular chondrocytes express a single immotile primary cilium [11]; a microtubule- based organelle that relies heavily on intraflagellar transport (IFT) proteins, including IFT88, which is part of the anterograde (towards ciliary tip) trafficking IFT-B complex. The primary cilium has a key role in Hh signaling; components of the pathway localising to the ciliary membrane and lack of a cilium prevents modulation of signaling. It is also directly linked with other growth factors signalling pathways such as TGFβ signaling [12], but also directly or indirectly with a large, and growing, list of signaling pathways [13].

The primary cilium has also been coined a ‘mechanosensor’, bending in response to fluid flow within the kidney, initiating downstream signaling pathways [14]. *In vitro* experiments in chondrocytes have implicated ciliary IFT88 both with compression-induced production of extracellular matrix proteins [15] and impaired clearance of aggrecanases, resulting in exacerbated degradation of aggrecan [16].

Developmental mutations in ciliary genes, including IFT88, result in impaired embryonic patterning arising from disrupted Hh signaling [17]. In addition, cartilage specific deletion of IFT88 results in disrupted long bone and articular cartilage formation [18]. The cartilage-specific deletion of a retrograde (towards cell body) ciliary IFT protein, IFT80, in the first 2 weeks of post-natal life, resulted in thicker articular cartilage [19]. Very little is directly known about the post-developmental influence of ciliary IFT beyond epiphysis formation.

We hypothesised that, ciliary IFT88 retains a crucial role in mediating adult cartilage homeostasis. Here we describe its importance in maturing and adult cartilage, and explore its role as a cellular mechano-regulator *in vivo* after pathological (joint destabilization) and physiological (voluntary wheel running) loading.

Results

Deleting IFT88 in adolescent chondrocytes results in thinner articular cartilage

To confirm location of Cre recombination, the *AggrecanCreER^{T2}* was crossed with a TdTomato reporter line. This identified Cre recombination in chondrocytes located in surface of hip articular cartilage (Supplementary Fig. 1A), all articular cartilage plateaus of the knee and in menisci (n=3) (Fig. 1A).

Median tibial articular cartilage thickness on the medial plateau remains statistically significantly thicker than lateral plateau cartilage throughout adolescence and adulthood (****p<0.0001) (Fig. 1B). Deletion of IFT88 was conducted at 4 or 6 weeks, with analysis 2 weeks later (Fig. 1C). When cartilage thickness of both lateral and medial plateaus were averaged, deletion at 6 weeks of age resulted in statistically significantly reduced cartilage thickness (95.58µm, 95% CI [92.08, 99.68] in control to 82.96µm, 95% CI [81.13, 91.56] in *AggrecanCreER^{T2};Ift88$^{fl/fl}$* mice). No such effect was observed when IFT88 was deleted at 4 weeks of age (Supplementary Fig. 1B). Considering each plateau separately, deletion of IFT88 resulted in statistically significantly reduced medial cartilage thickness at 6 weeks (median thickness 102.42µm 95% CI [91.7, 109.7] in control and 94.25µm; 95% CI [78.74, 101.3] in *AggrecanCreER^{T2};Ift88$^{fl/fl}$* mice) and at 8 weeks of age (median thickness 102.57µm 95% CI [94.3, 119.8] in control, 87.36µm 95% CI [81.35, 90.97] in *AggrecanCreER^{T2};Ift88$^{fl/fl}$* mice) (Fig. 1D and E). Lateral cartilage thickness was unaffected (Fig. 1D).

IFT88 deletion at 6 weeks of age leads to thinner calcified articular cartilage.

Thickness measurements of non-calcified and calcified regions were taken using the tidemark from Safranin O stained histological sections (Fig. 2A). The ratio of calcified to non-calcified articular cartilage shifted from 75% non-calcified at 4 weeks of age to 40% non-calcified cartilage by 22 weeks of age (Supplementary Fig. 2A) in control mice. Deletion of IFT88 resulted in thinner calcified cartilage regions; calcified cartilage median thickness at 6 weeks of age (37.52µm 95% CI [29.71, 45.17] in control, 29.96µm 95% CI [15.46, 34.50] in *AggrecanCreER^{T2};Ift88$^{fl/fl}$*) and at 8 weeks of age (48.43µm 95% CI [43.62, 54.64] in control, 41.29µm 95% CI [34.93, 44.17] in *AggrecanCreER^{T2};Ift88$^{fl/fl}$*). Non-calcified cartilage thickness was not statistically significantly different between control and *AggrecanCreER^{T2};Ift88$^{fl/fl}$* (Fig. 2B). Separation of measurements by lateral and medial plateaus revealed reductions in calcified cartilage were consistent across both plateaus, at both timepoints, albeit statistically significant only on the medial plateau between 6 and 8 weeks of age (Fig. 2C and 2D). Histological measurements of the subchondral bone revealed an increase in median subchondral bone thickness between 6 and 8 weeks of age in control mice, that was not affected by deletion of IFT88 (Fig. 2E and Supplementary Fig. 2B).

Deletion of IFT88 at 8 weeks of age results in atrophy of articular cartilage, associated with reduced calcified cartilage

Next, we administered tamoxifen at 8 weeks of age and collected joints 2, 14 or 26-weeks later at 10, 22 and 34-weeks of age respectively (Fig. 3A). Deletion of IFT88 resulted in 10-20% thinner tibial cartilage at every time point (Fig. 3B and C). Thinning did not appear to be cumulative over time and occurred without obvious surface fibrillation, thus indicative of “atrophy” rather than “degeneration” [3, 5, 20, 21]. Thinning was statistically significant at every time point on the medial plateau. By 34-

weeks of age, median thickness dropped from 104.00µm (95% CI [100.30, 110.50]) in control to 89.42µm (95% CI [84.00, 93.49]) in *AggrecanCreER^{T2};Ift88$^{fl/fl}$* (Fig. 3D). The effects were more modest on the lateral plateaus, where thinning was not apparent until 22-weeks of age (Supplementary Fig. 3A). Deletion of IFT88 did not statistically significantly affect non-calcified cartilage thickness on either plateau (Fig. 3E and Supplementary Fig. 3B). Statistically significant reductions in calcified cartilage thickness were observed on both the medial (58.72µm, 95% CI [54.34, 65.05]) in control to 45.62µm, 95% CI [39.32, 52.49]) in *AggrecanCreER^{T2};Ift88$^{fl/fl}$* (Fig. 3E) and lateral (Supplementary Fig. 3C) plateaus.

Atrophy of the medial cartilage predisposes joints to spontaneous osteoarthritis

At 34 weeks of age, *AggrecanCreER^{T2};Ift88$^{fl/fl}$* mice developed spontaneous medial compartment cartilage damage associated with osteophyte formation, together indicating development of osteoarthritis (Fig. 4A). OARSI scoring revealed no differences in disease scores before 22 weeks of age (Supplementary Fig. 4A), but a statistically significant increase in disease scores at 34 weeks (Fig. 4B). The highest OARSI scores were found on the medial plateau (Fig. 4C). There was no difference in osteophyte scores unless severe cartilage disease was recorded (Fig. 4D and Supplementary Fig. 4C)**.** This suggests IFT88 is chondroprotective possibly by optimising the cartilage thickness that protects mice from age-related osteoarthritis. By 34 weeks of age, thinning of subchondral bone was observed in *AggrecanCreER^{T2};Ift88$^{fl/fl}$* animals compared with controls on every plateau (Fig. 4F and Supplementary Fig. 4D). Epiphysis BV/TV (trabecular bone mineral density) was not affected (Supplementary Fig. 4E).

Deletion of IFT88 exacerbates osteoarthritis severity after surgical joint destabilisation

Supraphysiological mechanical loads, such as those experienced during and following a joint destabilising injury, drive OA development. Mice were given tamoxifen at 8 weeks of age, and surgical destabilisation of the medial meniscus (DMM) was performed at 10 weeks. At 8 or 12-weeks post-surgery, animals were culled and joints collected, along with respective Sham operated mice (Fig. 5A). Coronal histological sections (Fig. 5B) were assessed using summed OARSI scoring. Deletion of IFT88 resulted in exacerbated disease, as indicated by statistically significantly increased disease scores, at 12-weeks post-DMM (*Ift88$^{fl/fl}$* 22.08$\pm$ 9.30, *AggrecanCreER^{T2};Ift88$^{fl/fl}$* 29.83$\pm$ 7.69, $p<0.05$, n= 15 for both groups) but not 8-weeks post-DMM (*Ift88$^{fl/fl}$* 19.55$\pm$ 8.28, *AggrecanCreER^{T2};Ift88$^{fl/fl}$* 24.06$\pm$ 6.86, p=0.46, n= 14 and 12 respectively) (Fig. 5C). No differences in osteophyte size (Fig. 5D and Supplementary Fig. 5A), maturity or staining (Supplementary Fig. 5B-E) were observed between control and *AggrecanCreER^{T2};Ift88$^{fl/fl}$* animals at either time-point post-DMM. There was also no difference in BV/TV between control and *AggrecanCreER^{T2};Ift88$^{fl/fl}$* epiphyses 12-weeks following DMM (Supplementary Fig. 5F).

Articular cartilage atrophy and/or Ift88 expression does not associate/correlate with indicators of matrix catabolism, Hh activation or chondrocyte hypertrophy.

In order to investigate whether deletion of IFT88 increased catabolism of aggrecan *in vivo*, unstained tissue sections of control and *AggrecanCreER^{T2};Ift88$^{fl/fl}$* joints were

stained for the ADAMTS-4 and 5-generated, aggrecan neoepitope using an antibody raised against the synthetic epitope NITEGE [22] and thresholded to IgG control (Supplementary Fig. 6B). No discernible differences in neoepitope staining were observed comparing *AggrecanCreER^{T2};Ift88$^{fl/fl}$* joints at 10 or 22 weeks of age on either the medial (Fig. 6A) or lateral plateaus. Similarly, no difference in type X collagen (COLX) expression, a marker of Hh-driven chondrocyte hypertrophy [23], was observed by immunohistochemistry following deletion of IFT88 (Fig. 6B and IgG control Supplementary Fig. 6C).

RNA was isolated from micro-dissected articular cartilage (Supplementary Fig. 6A) from 10-week old control and *AggrecanCreER^{T2};Ift88$^{fl/fl}$* animals, 2 weeks after tamoxifen treatment. 44 candidate genes, associated with chondrocyte pathophysiology and/or implicated in primary ciliary signalling, were measured by qPCR. Using the spread of *Ift88* expression in control and *AggrecanCreER^{T2};Ift88$^{fl/fl}$* cartilage we correlated expression levels of each target following normalisation to the average of two housekeeper genes, *Hprt* and *Gapdh* (See Supplementary Table 1 for all genes). *Tcf7l2* was the only gene to be found statistically significantly correlated with *Ift88* expression after Bonferroni correction (corrected p value = cp; (p= 0.0006, cp=0.026, r^2= 0.8811) (Fig. 6C). However, *Ctgf*, *Gli2* and *Enpp1* were also positively correlated with *Ift88* expression before correction (p=0.002, p=0.0037, and p=0.009 respectively). *Ift88* gene expression was not correlated with *Adamts4*, *Adamts5* or *Colx* expression in line with our immunohistochemistry findings (Fig. 6A and 6B). *Timp3* was found to be weakly correlated with *Ift88* expression (p= 0.0189, cp=0.83). Additionally, *Acan,* and *Tgfbr3* were found to be positively correlated with *Ift88* before correction (p= 0.0124 and p= 0.0107 respectively). Importantly, expression of *Gli-1* and *Ptch-1,* indicators of Hh pathway activation, were not correlated with *Ift88* expression (Supplementary Table 1).

Medial articular cartilage atrophy in *AggrecanCreER^{T2};Ift88$^{fl/fl}$* is rescued by wheel exercise.

Mice were given free access to wheel exercise for two weeks immediately following tamoxifen injection at 8 weeks of age. Previously, two weeks was sufficient to measure a change in cartilage thickness in 'naïve' mice. We showed medial cartilage thinning in 'naïve' mice at 10 weeks of age in *AggrecanCreER^{T2};Ift88$^{fl/fl}$* mice. However, if mice had access to a wheel over the same time period, medial cartilage thinning was not observed (Fig. 6D and Supplementary Fig. 6D). Exercise had no effect on average cartilage thickness in control mice, but caused an increase in maximum thickness (Fig. Supplementary Fig. 6D).

Discussion

This study aimed to test the *in vivo* influence of ciliary IFT88 in post-natal articular cartilage by depleting its expression in chondrocytes *in vivo*. Previous mouse studies, using congenital mutations [24] or constitutive deletions of IFT88, demonstrated that joint development [18] and developmental dynamics in the wider musculoskeletal (MSK) system [17], are reliant on the activity of IFT88, most likely through regulation of Hh signalling [25], but also through cooperation with or regulation of Wnt, cytoskeletal organisation, polarity and/or the regulation of cellular response to mechanical loading. Other models targeting ciliary proteins such as KIF3A, BBS, and IFT80 also point to a role of the ciliary machinery in MSK development [19, 23, 26] that is further emphasised by the skeletal ciliopathies [27, 28]. Ciliary-regulated Hh signalling largely switches off in adulthood beyond progenitor cell populations [29], although may become reactivated in OA [8], again interacting with Wnt and other signalling pathways via TCF7L2 [30]. The broader question of how chondrocytes and/or cartilage integrate mechanical cues, evidently important to cartilage health, is, in adulthood, still open to debate, with a number of putative sensors or transducers, including primary cilia, proposed [31]. It remained unclear as to what the *in vivo* role of ciliary IFT was in adulthood.

The direct role of the primary cilium in MSK development is largely inferred from multiple knockouts and is very hard to address *in vivo*. *In vitro* hypomorphic mutation of IFT88 disrupts chondrocyte mechanotransduction in an ATP - Ca^{2+} - proteoglycan axis, but not mechanosensation [15], Hh transduction [32] and the response to inflammatory, osmotic, and other biophysical cues [33-35]. Activation of Hh *in vitro,* in the absence of many of these cues, has no effect on cartilage matrix turnover in tissue culture models [36], suggesting that *in vivo* matrix disruption, after interfering with the primary cilium, may not be through Hh signalling alone [37]. Further, the cilium has also been associated with integrins [38], TRPV4 [39] and other putative mechanosensitive molecules or channels. Collectively, these studies point to roles for the primary cilium in the response to biophysicochemical stimuli but with little direct, *in vivo* data to support this.

The principal aim therefore was to establish the *in vivo* influence of ciliary IFT88. We chose to induce deletion of IFT88 in chondrocytes from 4 weeks of age. We used a Cre recombinase driven by the aggrecan promotor to maintain expression through adulthood, in contrast with Col2a which largely switches off expression after skeletal maturity [40]. Crossing the *AggrecanCreER^{T2}* with a tomato reporter enabled post-natal visualisation of mosaic Cre recombination in the target articular cartilage of the knee. Within hip articular cartilage, qPCR suggested partial deletion which we interpret from the use of the reporter to be likely due to activity being limited to articular chondrocytes, and not hypertrophic chondrocytes (in the hip). Deletion of IFT88 in primary rib chondrocytes isolated from both *AggrecanCreER^{T2};Ift88$^{fl/fl}$* (cKO) and *ROSA26CreER^{T2};Ift88$^{fl/fl}$* mouse lines at 4 weeks of age, indicated similar deletion *in vitro*, higher deletions were achieved in kidney and liver tissue isolated from *ROSA26CreER^{T2};Ift88$^{fl/fl}$* (data not shown). A limitation of this study is the incomplete deletion of *Ift88*. The tomato reporter implies deletion is unlikely to take place in all chondrocytes but activation is not regionally biased in chondrocytes of the knee. Moreover, to fully address the question of whether primary cilia have been perturbed

as a result of IFT88 deletion in adult articular cartilage poses challenges related to staining of cilia, and difficulties in imaging cilia depending on their *in situ* orientation with respect to the optical plane.

A strength of this study is the robustness of the phenotype generated from mosaic IFT88 deletion, which was observed over two years of study, in over 70 animals, from multiple generations. A measurable thickness phenotype developed in *AggrecanCreER^{T2};Ift88$^{fl/fl}$* animals within 2 weeks. Thinning, ~10% on average, of articular cartilage was most marked on the medial plateau. We speculate this effect is largest on the thicker medial plateau, as thickness is mechanically defined [6], in a manner perhaps analogous to the bone 'mechanostat' proposed by Frost in 1987 [41] and designed to ensure chondrocytes experience forces in a narrow window [1]. The recovery of medial thinning in response to exercise, is conducive with, but does not prove, the possibility that ciliary IFT88 is a component of the cartilaginous response to mechanical inputs and important to adolescent and adult mechanoadaptation, as proposed first in the context of epithelial response to renal flow [14, 42], aberrant in polycystic kidney disease [43]. Loss of articular cartilage thickness was largely attributable to reductions in calcified cartilage. During adolescent cartilage maturation, deletion of IFT88 inhibited the gradual calcification of cartilage observed in control animals, particularly on the medial plateau. Deletion at 8 weeks of age resulted in diminished calcified cartilage within two weeks and led to subsequent further thinning in a manner analogous to tissue atrophy, without cartilage fibrillation commonly seen in disease models [5, 20, 21, 44]. This did not lead to increased subchondral bone thickness or alter the density (BV/TV) of the epiphysis, suggesting that calcified cartilage was not being converted to the bone beneath.

Up to 22 weeks of age cartilage atrophy did not progress and was not associated with spontaneous cartilage fibrillation or higher OARSI scores. However, at 34 weeks of age, deletion of IFT88 resulted in full medial loss of cartilage associated with osteophytes and higher OARSI scores in some mice. With the inherent loss of cartilage thickness, it was not surprising that joints were pre-disposed to higher disease scores 12 weeks post-DMM, albeit not at 8 weeks post-DMM. The removal of IFT88 therefore appears to be important in protecting against otherwise pathophysiological mechanical inputs, but this protection is not extended to DMM mechanics.

We previously linked IFT88 to aggrecanase activity *in vitro* [16], but here found no correlations in gene expression to link observed atrophy to altered expression of proteases or LRP-1 (receptor for protease clearance). There were also no apparent increases in aggrecanase-mediated aggrecan neoepitope *in situ*. However, both *Acan* (aggrecan) and an inhibitor of metalloproteinase activity, *timp3,* correlated with IFT88 expression, and we cannot yet conclude whether increased catabolism or failed anabolism is the cause of atrophy. We found no changes in COLX protein expression, associated with deeper zones of cartilage, between *AggrecanCreER^{T2};Ift88$^{fl/fl}$* and control mice. Additionally, no correlations at the level of mRNA between *Ift88* and *Colx* or other hypertrophic markers in cartilage/bone interface (Supplementary Table 1) were identified. Calcification of cartilage in the mouse has recently been linked to both Hh and ENPP1, a pyrophosphatase [45]. Expression of *Enpp1* positively correlated

with *Ift88* in microdissected articular cartilage. Many genes measured were not correlated to *Ift88*. Importantly, genes associated with Hh signalling, including pathway activation status, were not correlated or apparently activated in *AggrecanCreER^{T2};Ift88$^{fl/fl}$* mice (Supplementary Table 1).

Our *in situ* molecular screen did find the transcription factor *Tcf7l2*, previously shown to influence and interact with Hh and β-catenin signalling pathways in cartilage [30], positively correlated with *Ift88* expression at 8 weeks of age, as did *Ctgf*. In cartilage CTGF is covalently bound to latent TGFβ and controls its bioavailability through the cell surface receptor TGFβR3. CTGF deletion results in thickening of articular cartilage although this was thought to be due to compensation by another TGFβ family member (Vincent, unpublished) [9]. *Tgfbr3* also positively correlated with *Ift88* expression in this experiment (Supplementary Table 1).

Intriguingly, we found exercise rescued the atrophy seen in *AggrecanCreER^{T2};Ift88$^{fl/fl}$* mice, whilst exercise had a modest effect on wild type mice; having no effect on average thickness, but causing an increase in maximum thickness (Supplementary Fig. 6D). This suggests either an IFT88-independent, mechanically-induced signal compensates for the loss of IFT88 and/or that IFT88 is a regulator of specific, mechanically-activated signals. It is also possible that there is a cartilage thickness ceiling effect; meaning that it is simply easier to measure an increase in thickness of cartilage with wheel exercise when the cartilage is thinner, as observed in atrophy. This functionally significant interaction between IFT88, and possibly therefore the primary cilium, and a mechanical load-driven post-natal tissue response may involve *Tcf7l2* and potentially TGFβ signalling, but these, along with other putative molecular pathways such as the IFT88-dependent induction of CITED [46], need to be investigated further.

In summary, these data demonstrate, unequivocally, that IFT88 remains highly influential in adolescent and adult articular cartilage as a positive regulator of cartilage thickness. IFT88 is important in the calcification of cartilage through early adulthood and is chondroprotective, with its loss resulting in atrophy of the tissue, predisposing to osteoarthritis over time. IFT88 loss is not associated with obvious activation of proteases nor Hh signalling activity, but cartilage atrophy, downstream to its removal, is reversed by exercise, suggesting a role for IFT88 in the maintenance of cartilage thickness downstream of physiological mechanical load.

Materials and Methods

Animals: All mice were housed in the biomedical services unit (BSU) at the Kennedy Institute, within the University of Oxford. Mice were housed 4–7 per standard, individually-ventilated cages and maintained under 12-h light/12-h dark conditions at an ambient temperature of 21°C. *Ift88*$^{fl/fl}$ mice were obtained from Jackson labs (Stock No. 022409) and maintained as the control line, and in parallel offspring were crossed with the *AggrecanCreER*^{T2} mouse line, *AggrecanCreER*^{T2}*;Ift88*$^{fl/fl}$ (Ift88 cKO), originally generated at the Kennedy Institute of Rheumatology [47]. The TdTomato reporter mouse line *B6.Cg-Gt(ROSA)26Sor*$^{tm14(CAG-TdTomato)Hze}$*/J* was originally from Jackson Laboratories (Stock No. 007914).

Tamoxifen treatment: Tamoxifen (Sigma-Aldrich, catalog no. T5648) was dissolved in 90% sunflower oil and 10% ethanol at a concentration of 20mg/ml by sonication. Tamoxifen was administered via intraperitoneal injection at ages according to experimental requirement, on three consecutive days at 50-100mg/kg (dependent on animal weight). For wheel exercised mouse experiments, animals had access to a wheel for two weeks following tamoxifen at 8 weeks of age.

Destabilisation of the medial meniscus (DMM): Mice were given tamoxifen 2 weeks prior to surgery. Male *Ift88*$^{fl/fl}$ *(control)* and *AggrecanCreER*^{T2}*;Ift88*$^{fl/fl}$ mice underwent DMM surgery at 10 weeks of age as previously described [48] or capsulotomy as Sham surgery. Mice were culled 8 or 12-weeks post-DMM. Mice were anaesthetised as described previously [22].

Histology: Knee joints were harvested into 10% neutral buffered formalin (CellPath, Newtown, UK) for 24-48 hours. Joints were decalcified (EDTA), paraffin embedded, coronally sectioned through the entire depth of the joint. Sections, at 80µm intervals were stained with Safranin O.

OARSI scoring: Safranin O stained joint sections were assessed by a degradative cartilage scoring system, as previously described [48], by 2 blinded observers. Summed score method (sum of 3 highest scores given per section for any joint, with a minimum of 9 sections per joint) was used.

Osteophyte quantification: Osteophyte size, maturity, and loss of medial tibial cartilage proteoglycan staining was assessed on a 0-3 scale as described previously [49].

Cartilage thickness measurements: To assess cartilage thickness in the joint, the average of three measurements per tibial plateau, from three consecutive sections from the middle of the joint was used (18 measurements). The same method was used to measure non-calcified cartilage thickness in the same location as the total cartilage thickness measurement. To find calcified cartilage, non-calcified cartilage length was taken away from total cartilage length. All images were double-scored by independent researchers. All measurements were performed using imageJ (Supplementary Fig. 2C).

Subchondral bone measurements: Subchondral bone measurements were taken as previously described [50]. Briefly, using ImageJ, five measurements were taken perpendicular to the articular cartilage plateau, from the chondro-osseous junction to the top of bone marrow or to the growth plate if there was no bone marrow. Mean measurements were calculated for each plateau and knee. Subchondral bone thickness was measured from at least 3 sections of each plateau of each knee (Supplementary Fig. 4D).

MicroCT BV/TV: Knee joints were imaged using a MicroCT scanner (SkyScan1172 X-ray microtomograph, Antwerp, Belgium) within 70% ethanol (10μm/pixel, 3 minutes of acquisition time). Using the CTan (Brucker Belgium) programme, saved image sequences were opened in the software to conduct 3D parameter analysis. Regions of interest were defined and used to calculate the bone volume (BV), total volume (TV), ratio of BV to TV (BV/TV).

Immunohistochemistry: Fixed, decalcified, unstained coronal knee sections were deparaffinised, rehydrated, quenched in 0.3M glycine and treated with proteinase K for 10 minutes. Samples underwent chondroitinase (0.1U) treatment for 30mins at 37ºC blocked in 5% goat serum and 10% bovine serum albumin (BSA) in phosphate-buffered saline, and were permeabilised by 0.2% Triton X-100 for 15mins. Samples were incubated with primary antibody (anti-ColX, 1:50, Abcam, catalog no. ab58632, anti-NITEGE, 1:50, Thermo Scientific, catalog no. PA1-1746, IgG (1:50) control, or no primary) overnight at 4ºC. Sections were washed and incubated with alexa-conjugated 555 secondary antibodies for 30 mins. Samples were incubated with nuclear stain DAPI (1:5000), before mounting in Prolong Gold and visualised**.**

RNA extraction: Articular cartilage was micro-dissected using a scalpel from the femoral and tibial plateaus of two animals (per n), and harvested directly into RNA*later* (Invitrogen). Samples were transferred to buffer RLT (Qiagen) and, using a scalpel, samples were diced further before pulverisation using a PowerGen 125 Polytron instrument (Fisher Scientific) for 3x 20 seconds with 10 second intervals. RNA of knee cartilage was isolated using the RNeasy Micro kit (Qiagen) and eluted into 14ul of nuclease free water and stored at -80 ºC until further analysis.

qPCR Using RNA isolated from micro-dissected knee cartilage, cDNA was synthesised (Applied Biosystems) and real-time quantitative PCR was performed using a Viia 7 Real-Time PCR System on 384 custom-made TaqMan microfluidic cards (ThermoFisher, catalog no. 4342253), according to the instructions of the manufacturer. Results were analysed to find fold change with respect to the average CT values of *Gapdh* and *Hprt* housekeeper genes. Linear regressions were used to correlate *Ift88* expression and subsequent raw p values and corrected (Bonferroni) calculated using GraphPad Prism 9.

References

1. Simon, W.H., *Scale effects in animal joints. I. Articular cartilage thickness and compressive stress.* Arthritis Rheum, 1970. **13**(3): p. 244-56.
2. Grodzinsky, A.J., et al., *Cartilage tissue remodeling in response to mechanical forces.* Annu Rev Biomed Eng, 2000. **2**: p. 691-713.
3. Palmoski, M.J. and K.D. Brandt, *Effects of static and cyclic compressive loading on articular cartilage plugs in vitro.* Arthritis Rheum, 1984. **27**(6): p. 675-81.
4. Osborne, A.C., et al., *Short-term rigid and flaccid paralyses diminish growth of embryonic chick limbs and abrogate joint cavity formation but differentially preserve pre-cavitated joints.* J Musculoskelet Neuronal Interact, 2002. **2**(5): p. 448-56.
5. Palmoski, M., E. Perricone, and K.D. Brandt, *Development and reversal of a proteoglycan aggregation defect in normal canine knee cartilage after immobilization.* Arthritis Rheum, 1979. **22**(5): p. 508-17.
6. Vincent, T.L. and A.K.T. Wann, *Mechanoadaptation: articular cartilage through thick and thin.* J Physiol, 2018.
7. Vincent, T.L., et al., *Basic fibroblast growth factor mediates transduction of mechanical signals when articular cartilage is loaded.* Arthritis Rheum, 2004. **50**(2): p. 526-33.
8. Lin, A.C., et al., *Modulating hedgehog signaling can attenuate the severity of osteoarthritis.* Nat Med, 2009. **15**(12): p. 1421-5.
9. Tang, X., et al., *Connective tissue growth factor contributes to joint homeostasis and osteoarthritis severity by controlling the matrix sequestration and activation of latent TGFbeta.* Ann Rheum Dis, 2018.
10. Wu, Q., Y. Zhang, and Q. Chen, *Indian hedgehog is an essential component of mechanotransduction complex to stimulate chondrocyte proliferation.* J Biol Chem, 2001. **276**(38): p. 35290-6.
11. Poole, C.A., et al., *Confocal analysis of primary cilia structure and colocalization with the Golgi apparatus in chondrocytes and aortic smooth muscle cells.* Cell Biol Int, 1997. **21**(8): p. 483-94.
12. Bangs, F. and K.V. Anderson, *Primary Cilia and Mammalian Hedgehog Signaling.* Cold Spring Harb Perspect Biol, 2017. **9**(5).
13. Wheway, G., L. Nazlamova, and J.T. Hancock, *Signaling through the Primary Cilium.* Frontiers in Cell and Developmental Biology, 2018. **6**(8).
14. Praetorius, H.A., et al., *Bending the primary cilium opens Ca2+-sensitive intermediate-conductance K+ channels in MDCK cells.* J Membr Biol, 2003. **191**(3): p. 193-200.
15. Wann, A.K., et al., *Primary cilia mediate mechanotransduction through control of ATP-induced Ca2+ signaling in compressed chondrocytes.* Faseb j, 2012. **26**(4): p. 1663-71.
16. Coveney, C.R., et al., *Cilia protein IFT88 regulates extracellular protease activity by optimizing LRP-1-mediated endocytosis.* FASEB J, 2018: p. fj201800334.
17. Haycraft, C.J., et al., *Intraflagellar transport is essential for endochondral bone formation.* Development, 2007. **134**(2): p. 307-16.

18. Chang, C.F., G. Ramaswamy, and R. Serra, *Depletion of primary cilia in articular chondrocytes results in reduced Gli3 repressor to activator ratio, increased Hedgehog signaling, and symptoms of early osteoarthritis.* Osteoarthritis Cartilage, 2012. **20**(2): p. 152-61.
19. Yuan, X. and S. Yang, *Deletion of IFT80 Impairs Epiphyseal and Articular Cartilage Formation Due to Disruption of Chondrocyte Differentiation.* PLoS One, 2015. **10**(6): p. e0130618.
20. Benichou, C. and J.M. Wirotius, *Articular cartilage atrophy in lower limb amputees.* Arthritis Rheum, 1982. **25**(1): p. 80-2.
21. Palmoski, M.J. and K.D. Brandt, *Running inhibits the reversal of atrophic changes in canine knee cartilage after removal of a leg cast.* Arthritis Rheum, 1981. **24**(11): p. 1329-37.
22. Ismail, H.M., et al., *JNK2 controls aggrecan degradation in murine articular cartilage and the development of experimental osteoarthritis.* Arthritis Rheumatol, 2015.
23. Koyama, E., et al., *Conditional Kif3a ablation causes abnormal hedgehog signaling topography, growth plate dysfunction, and excessive bone and cartilage formation during mouse skeletogenesis.* Development, 2007. **134**(11): p. 2159-69.
24. McGlashan, S.R., et al., *Articular cartilage and growth plate defects are associated with chondrocyte cytoskeletal abnormalities in Tg737orpk mice lacking the primary cilia protein polaris.* Matrix Biol, 2007. **26**(4): p. 234-46.
25. Chang, C.F. and R. Serra, *Ift88 regulates Hedgehog signaling, Sfrp5 expression, and beta-catenin activity in post-natal growth plate.* J Orthop Res, 2013. **31**(3): p. 350-6.
26. Kaushik, A.P., et al., *Cartilage abnormalities associated with defects of chondrocytic primary cilia in Bardet-Biedl syndrome mutant mice.* J Orthop Res, 2009. **27**(8): p. 1093-9.
27. Huber, C. and V. Cormier-Daire, *Ciliary disorder of the skeleton.* Am J Med Genet C Semin Med Genet, 2012. **160c**(3): p. 165-74.
28. Wang, C., X. Yuan, and S. Yang, *IFT80 is essential for chondrocyte differentiation by regulating Hedgehog and Wnt signaling pathways.* Exp Cell Res, 2013. **319**(5): p. 623-32.
29. Petrova, R. and A.L. Joyner, *Roles for Hedgehog signaling in adult organ homeostasis and repair.* Development, 2014. **141**(18): p. 3445-57.
30. Rockel, J.S., et al., *Hedgehog inhibits β-catenin activity in synovial joint development and osteoarthritis.* J Clin Invest, 2016. **126**(5): p. 1649-63.
31. Drexler, S.K., Wann, A. K. T., Vincent, Tonia L, *Are cellular mechanosensors potential therapeutic targets in osteoarthritis.* International Journal of Clinical Rheumatology, 2014.
32. Clement, C.A., L.A. Larsen, and S.T. Christensen, *Using nucleofection of siRNA constructs for knockdown of primary cilia in P19.CL6 cancer stem cell differentiation into cardiomyocytes.* Methods Cell Biol, 2009. **94**: p. 181-97.
33. Wann, A.K., J.P. Chapple, and M.M. Knight, *The primary cilium influences interleukin-1beta-induced NFkappaB signalling by regulating IKK activity.* Cell Signal, 2014. **26**(8): p. 1735-42.
34. McFie, M., et al., *Ciliary proteins specify the cell inflammatory response by tuning NFκB signaling, independently of primary cilia.* J Cell Sci, 2020.

35. Anvarian, Z., et al., *Cellular signalling by primary cilia in development, organ function and disease.* Nat Rev Nephrol, 2019. **15**(4): p. 199-219.
36. Thompson, C.L., et al., *Hedgehog signalling does not stimulate cartilage catabolism and is inhibited by Interleukin-1beta.* Arthritis Res Ther, 2015. **17**: p. 373.
37. Collins, I. and A.K.T. Wann, *Regulation of the Extracellular Matrix by Ciliary Machinery.* Cells, 2020. **9**(2).
38. Knight, M.M., et al., *Articular chondrocytes express connexin 43 hemichannels and P2 receptors - a putative mechanoreceptor complex involving the primary cilium?* J Anat, 2009. **214**(2): p. 275-83.
39. Kottgen, M., et al., *TRPP2 and TRPV4 form a polymodal sensory channel complex.* J Cell Biol, 2008. **182**(3): p. 437-47.
40. Nagao, M., C.W. Cheong, and B.R. Olsen, *Col2-Cre and tamoxifen-inducible Col2-CreER target different cell populations in the knee joint.* Osteoarthritis Cartilage, 2016. **24**(1): p. 188-91.
41. Frost, H.M., *The mechanostat: a proposed pathogenic mechanism of osteoporoses and the bone mass effects of mechanical and nonmechanical agents.* Bone Miner, 1987. **2**(2): p. 73-85.
42. Nauli, S.M., et al., *Polycystins 1 and 2 mediate mechanosensation in the primary cilium of kidney cells.* Nat Genet, 2003. **33**(2): p. 129-37.
43. Yoder, B.K., et al., *Polaris, a protein disrupted in orpk mutant mice, is required for assembly of renal cilium.* Am J Physiol Renal Physiol, 2002. **282**(3): p. F541-52.
44. Nomura, M., et al., *Thinning of articular cartilage after joint unloading or immobilization. An experimental investigation of the pathogenesis in mice.* Osteoarthritis Cartilage, 2017. **25**(5): p. 727-736.
45. Jin, Y., et al., *Enpp1 inhibits ectopic joint calcification and maintains articular chondrocytes by repressing hedgehog signaling.* Development, 2018. **145**(18).
46. He, Z., et al., *Strain-induced mechanotransduction through primary cilia, extracellular ATP, purinergic calcium signaling, and ERK1/2 transactivates CITED2 and downregulates MMP-1 and MMP-13 gene expression in chondrocytes.* Osteoarthritis Cartilage, 2016. **24**(5): p. 892-901.
47. Lo Cascio, L., et al., *Generation of a mouse line harboring a Bi-transgene expressing luciferase and tamoxifen-activatable creER(T2) recombinase in cartilage.* Genesis, 2014. **52**(2): p. 110-9.
48. Glasson, S.S., et al., *Deletion of active ADAMTS5 prevents cartilage degradation in a murine model of osteoarthritis.* Nature, 2005. **434**(7033): p. 644-8.
49. Little, C.B., et al., *Matrix metalloproteinase 13-deficient mice are resistant to osteoarthritic cartilage erosion but not chondrocyte hypertrophy or osteophyte development.* Arthritis Rheum, 2009. **60**(12): p. 3723-33.
50. Nalesso, G., et al., *WNT16 antagonises excessive canonical WNT activation and protects cartilage in osteoarthritis.* Ann Rheum Dis, 2017. **76**(1): p. 218-226.

Figures

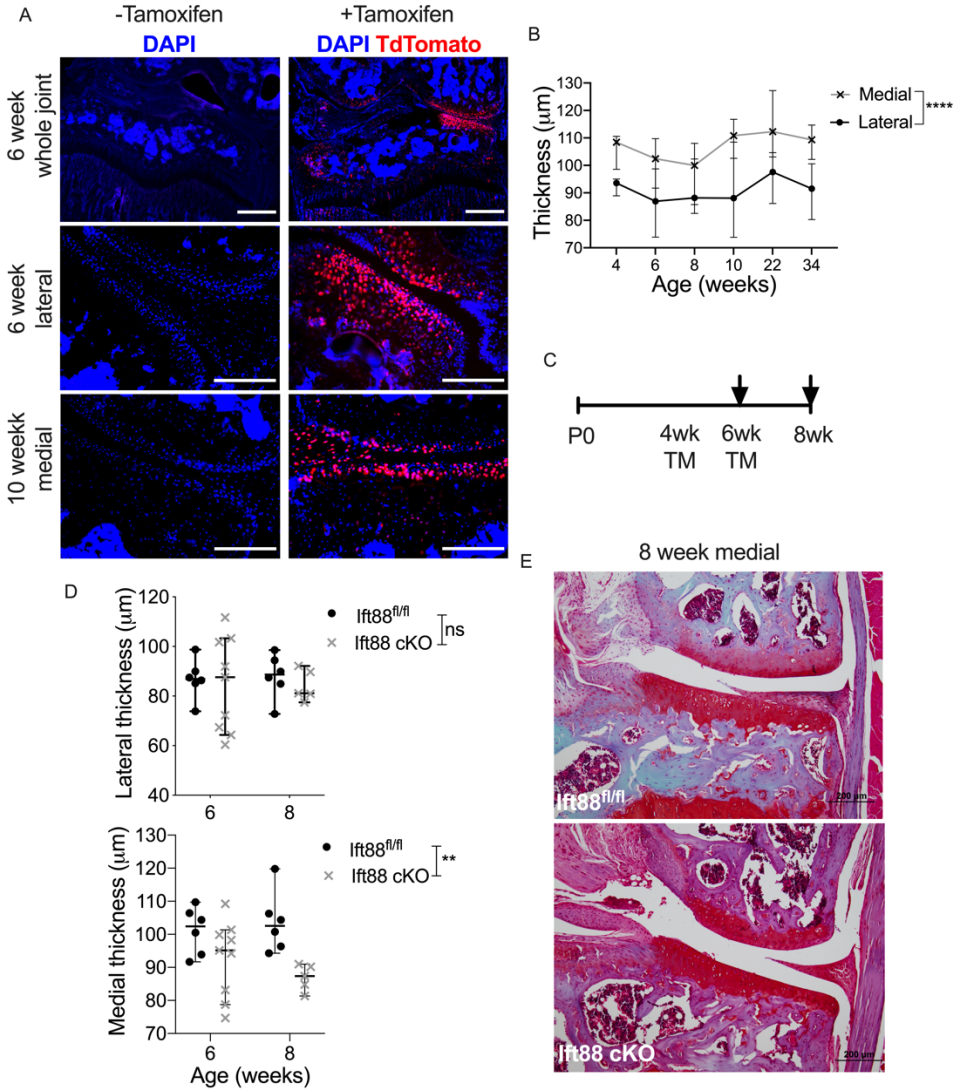

Figure 1. Deleting IFT88 in adolescent chondrocytes results in thinner articular cartilage. A, *AggrecanCreER^{T2}* animals were crossed with TdTomato reporter animals. Cryosections of knee joints were counterstained with nuclear stain DAPI. Animals received tamoxifen at 6 and 10-weeks of age, (scale bar= 200 µm). **B,** Median lateral and medial cartilage thickness from control animals at 4, 6, 8, 10, 22 and 34 weeks of age. **C,** Experimental schematic showing age of tamoxifen administration (TM) and collection. Arrows denote collection points. **D,** Lateral and medial cartilage thickness in control (*Ift88$^{fl/fl}$*) and *AggrecanCreER^{T2};Ift88$^{fl/fl}$* animals at 6 and 8 weeks of age. **E,** Safranin O stained images of representative 8-week old medial cartilage two weeks post-TM, (scale bar= 200 µm). Points represent median +/- 95% confidence intervals. Analysed by two-way ANOVA, **p<0.01, ****p<0.0001.

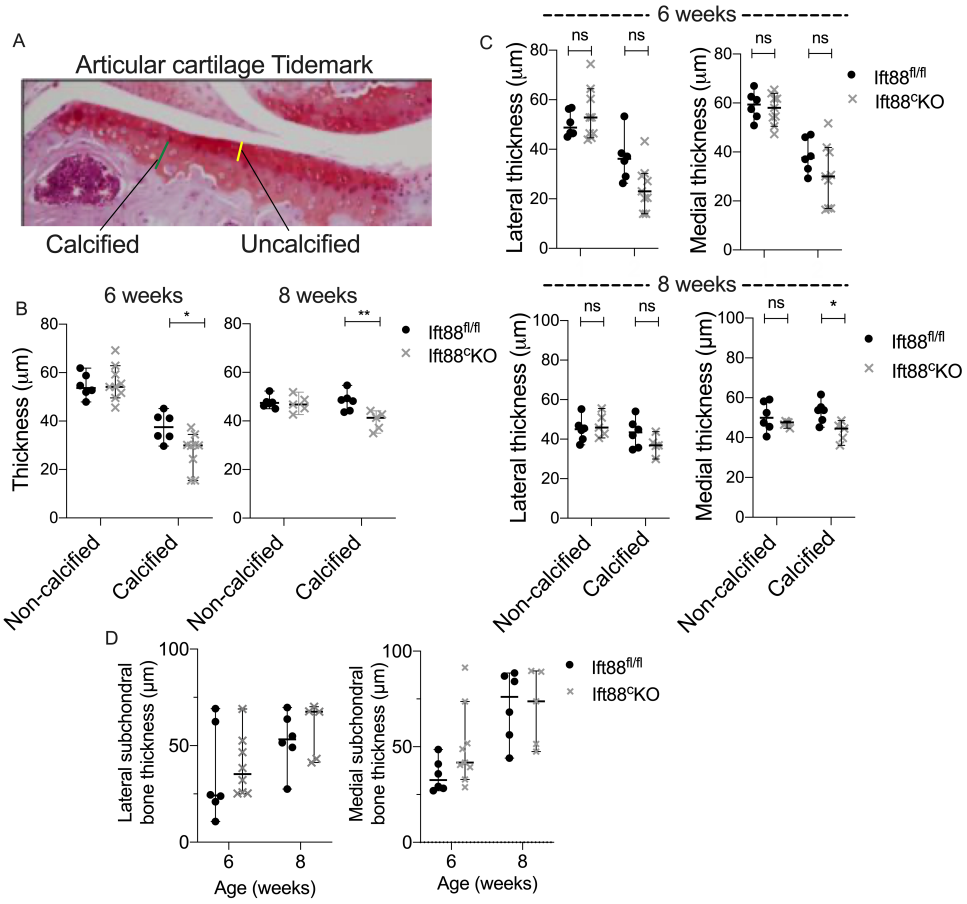

Figure 2. IFT88 deletion in adolescence leads to thinner calcified articular cartilage. A, Safranin O stained histological sections of articular cartilage showing non-calcified (yellow line) and calcified (green line) cartilage regions, demarcated by tidemark. **B,** Average of median medial and lateral non-calcified and calcified cartilage thickness at 6 and 8 weeks of age. **C,** Median non-calcified and calcified cartilage thickness of lateral and medial plateaus at 6 and 8 weeks of age. D**,** Median subchondral bone thickness in 6 and 8-week old joints on medial and lateral plateaus. Points represent median +/- 95% confidence intervals. Analysed by two-way ANOVA, *p<0.05, **p<0.01**.** Minimum n of 5 joints in any group.

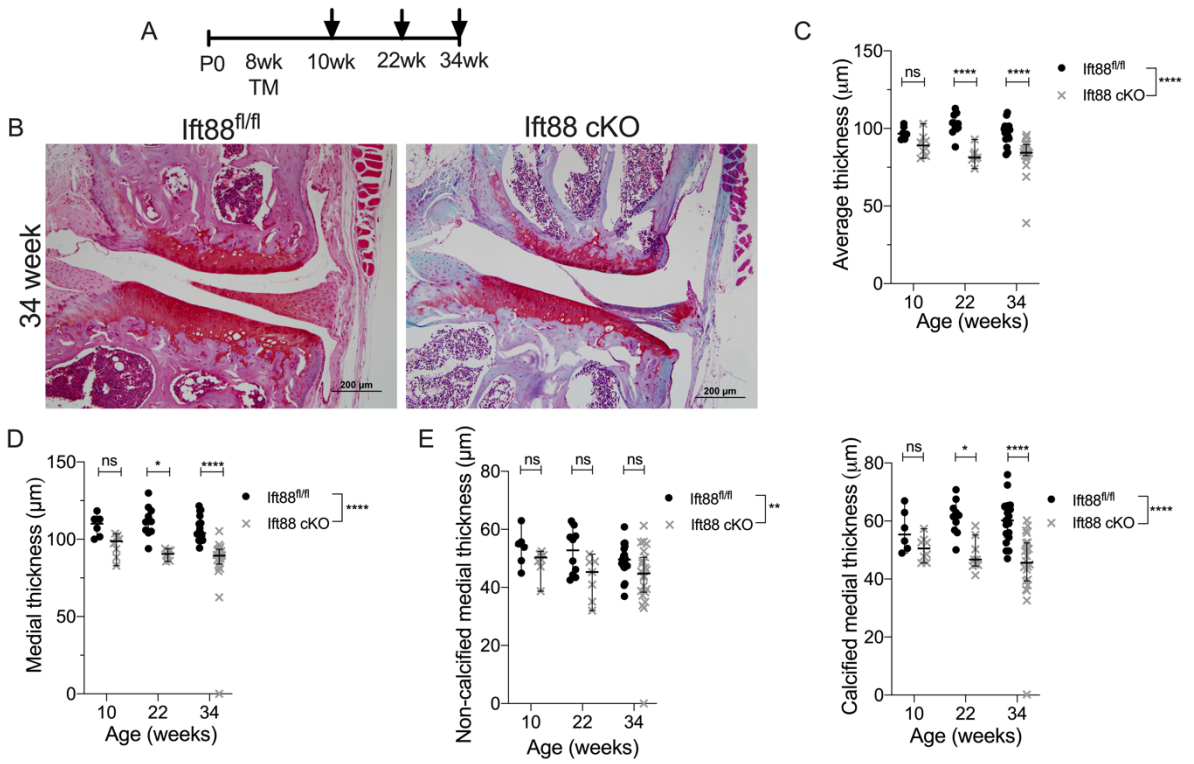

Figure 3. Deletion of IFT88 at 8 weeks of age results in atrophy of articular cartilage associated with reductions in calcified cartilage. A, Schematic representation of experimental timeline (TM= tamoxifen). Arrows denote collection points. **B,** Safranin O stained representative histological sections of medial compartment of 34-week old control and *AggrecanCreER^{T2};Ift88$^{fl/fl}$* animals (scale bar= 200 µm). **C,** Average of median (both compartments) cartilage thickness measurements of mice aged 10, 22 and 34 weeks of age. **D,** Medial cartilage thickness at 10, 22 and 34 weeks of age. **E,** Medial non-calcified and calcified cartilage thickness. Points represent median +/- 95% confidence intervals. Analysed by two-way ANOVA, **p<0.01, ***p<0.001, ****p<0.0001. 10 weeks, *Ift88$^{fl/fl}$* n= 6, *AggrecanCreER^{T2};Ift88$^{fl/fl}$* n=8; 22 weeks, *Ift88$^{fl/fl}$* n= 10, *AggrecanCreER^{T2};Ift88$^{fl/fl}$* n=7; 34 weeks, *Ift88$^{fl/fl}$* n= 19, *AggrecanCreER^{T2};Ift88$^{fl/fl}$* n=22.

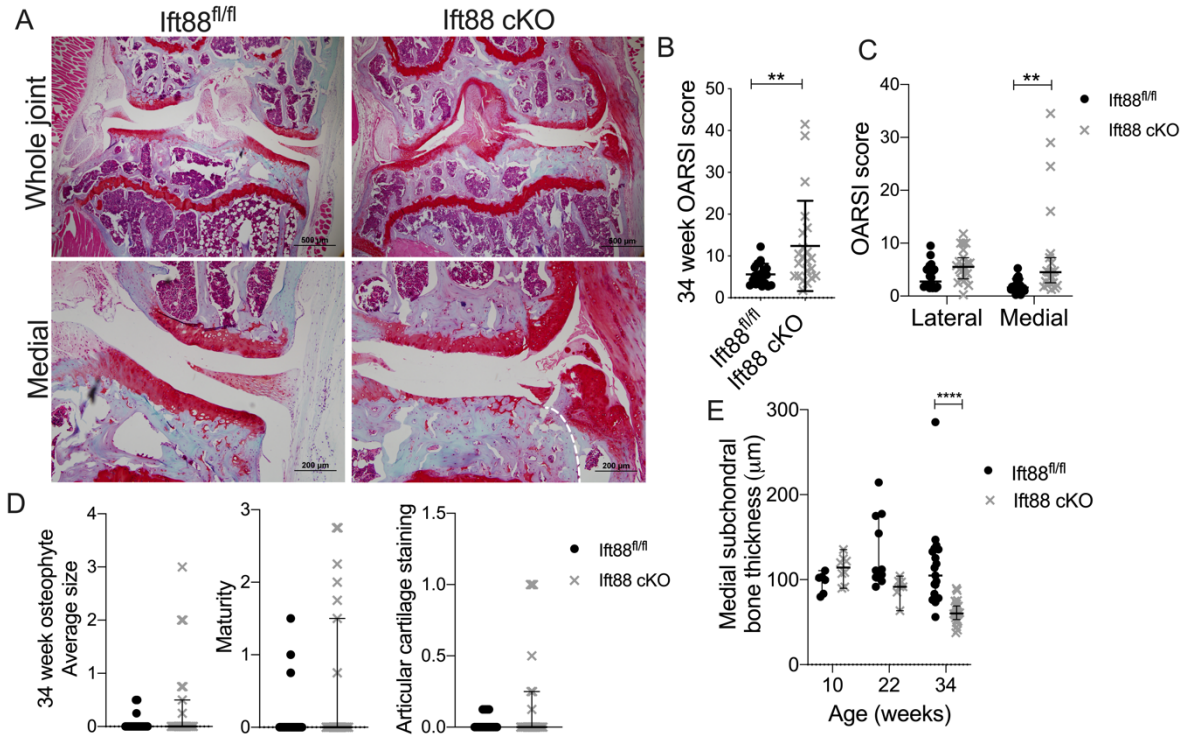

Figure 4. Spontaneous osteoarthritis in IFT88 *AggrecanCreER^{T2};Ift88$^{fl/fl}$* at 34 weeks of age. A, Safranin O stained histological sections of whole joint (scale bar= 500µm) and medial compartment (scale bar= 200µm) of 34-week old control and *AggrecanCreER^{T2};Ift88$^{fl/fl}$* animals. White dashed line demarcates formation of osteophyte. **B,** Summed modified OARSI scores in sections from 34-week old animals. Analysed by Mann-Whitney test, **p<0.01**. C,** Summed modified OARSI scores from lateral and medial plateaus in sections from 34-week old animals. **D,** Osteophyte size, osteophyte maturity, and staining of articular cartilage scores at 34 weeks of age. **E,** Medial subchondral bone thickness. 34 weeks: *Ift88$^{fl/fl}$* n= 19, *AggrecanCreER^{T2};Ift88$^{fl/fl}$* n=22. Points represent median +/- 95% confidence intervals. Analysed by two-way ANOVA unless stated otherwise, ****p<0.0001.

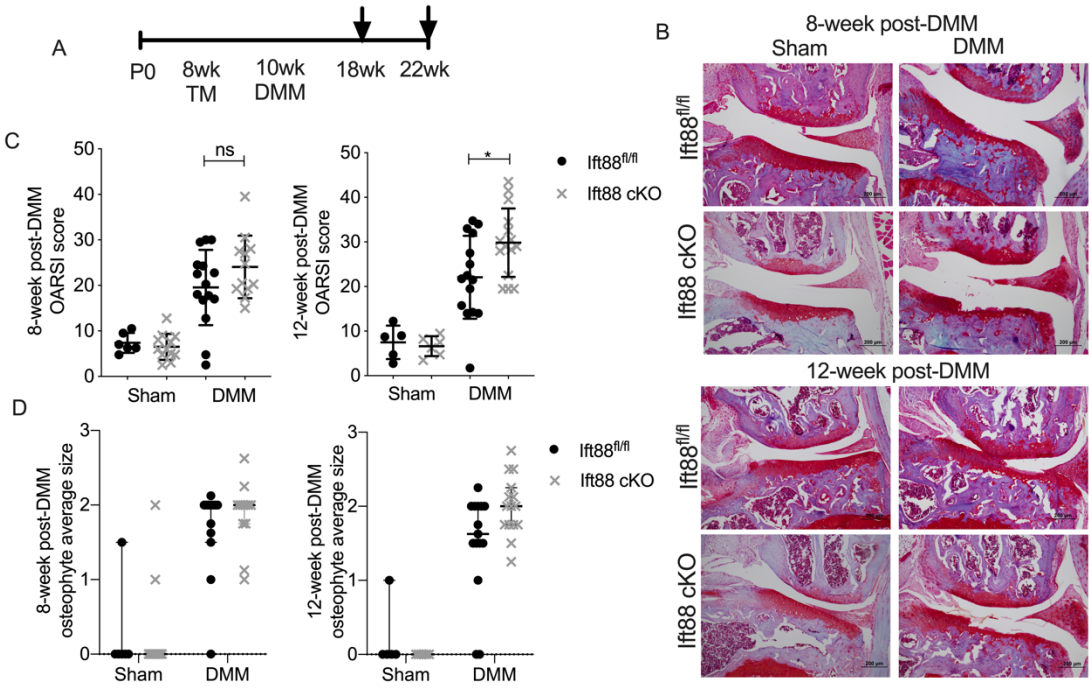

Figure 5. Deletion of IFT88 results in exacerbated disease 12 weeks after surgical destabilisation. A, Schematic representation of experimental timeline for DMM surgery (TM= tamoxifen). Arrows denote collection points. **B,** Safranin O stained histological sections of medial compartments from Sham and DMM animals operated animals 8 and 12-weeks post DMM surgery. Scale bars = 200µm. **C,** Summed modified OARSI scores in sections from Sham and DMM operated knees 8 and 12 weeks post-DMM. Minimum Sham surgeries in any group n= 5. **D,** Osteophyte average size 8 and 12 weeks post-DMM. 8 weeks post-DMM; *Ift88*$^{fl/fl}$ n= 14, *AggrecanCreER*^{T2}*;Ift88*$^{fl/fl}$ n=12. 12 weeks post-DMM; *Ift88*$^{fl/fl}$ n= 15, *AggrecanCreER*^{T2}*;Ift88*$^{fl/fl}$ = 15. Points represent median +/- 95% confidence intervals. Analysed by two-way ANOVA, *p<0.05.

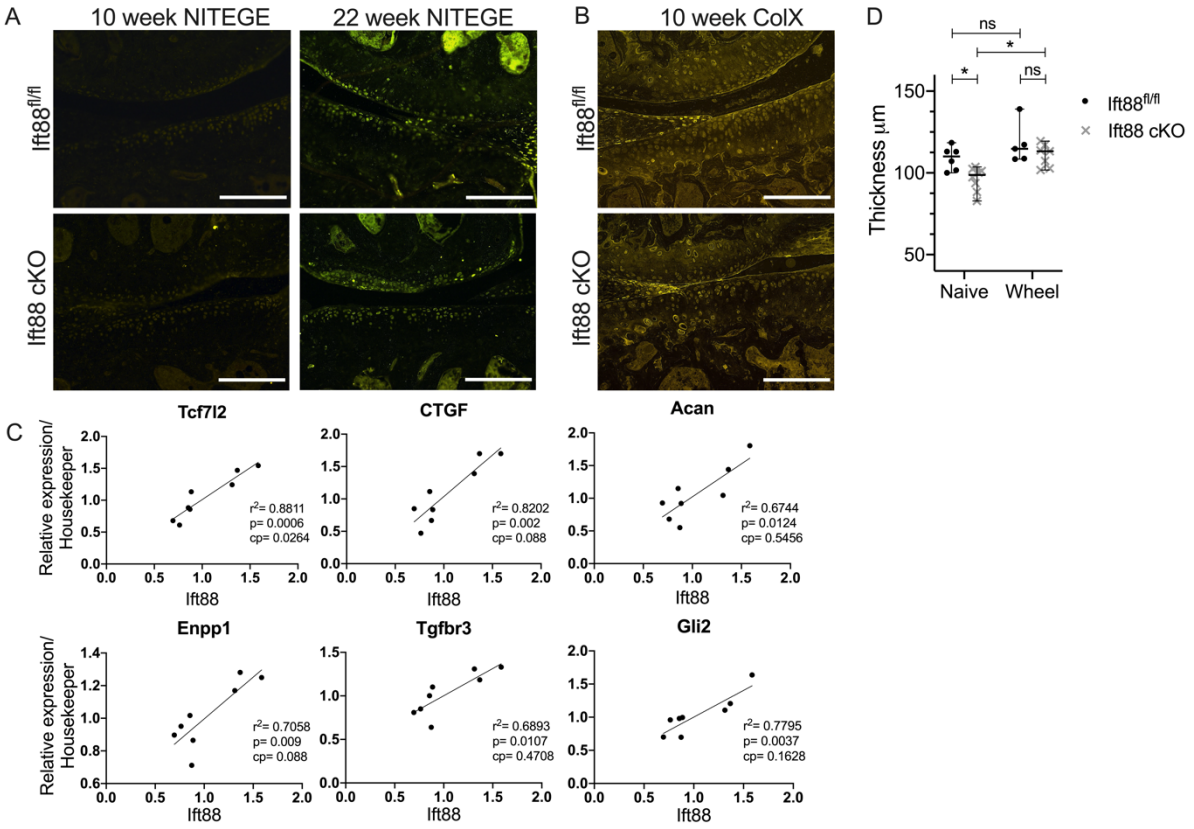

Figure 6. IFT88-induced atrophy is not associated with aggrecaneolysis, but *Ift88* is correlated to *Tcf7l2 and Ctgf* expression *in vivo and thickness is restored by exercise* . A, Representative immunofluorescent staining of aggrecan neoepitope NITEGE (n= 6 in all groups). Scale bars = 200µm. **B,** Representative immunofluorescent staining of type X collagen (n= 6 in all groups). Scale bars = 200µm. **C,** RNA extracted from micro-dissected articular cartilage was analysed by qPCR to identify genes correlating with *Ift88* expression following normalisation to *Gapdh* and *Hprt*. Linear regression was performed and statistical significance assessed following Bonferroni correction (cp= corrected p value). *Tcf7l2* positively correlated with IFT88 expression before and after correction (p= 0.0006, cp= 0.0264), whilst *Ctgf*, *Acan*, *Enpp1*, *Tgfbr3* and *Gli2* correlated positively before correction (see figure for p values of Supplementary Table 1). **D,** Median medial cartilage thickness in naïve (non-exercised) and wheel exercised mice. *Ift88$^{fl/fl}$* n= 5, *AggrecanCreER^{T2};Ift88$^{fl/fl}$* n=7. Points represent median +/- 95% confidence intervals. Analysed by two-way ANOVA, *p<0.05.

Supplementary figures

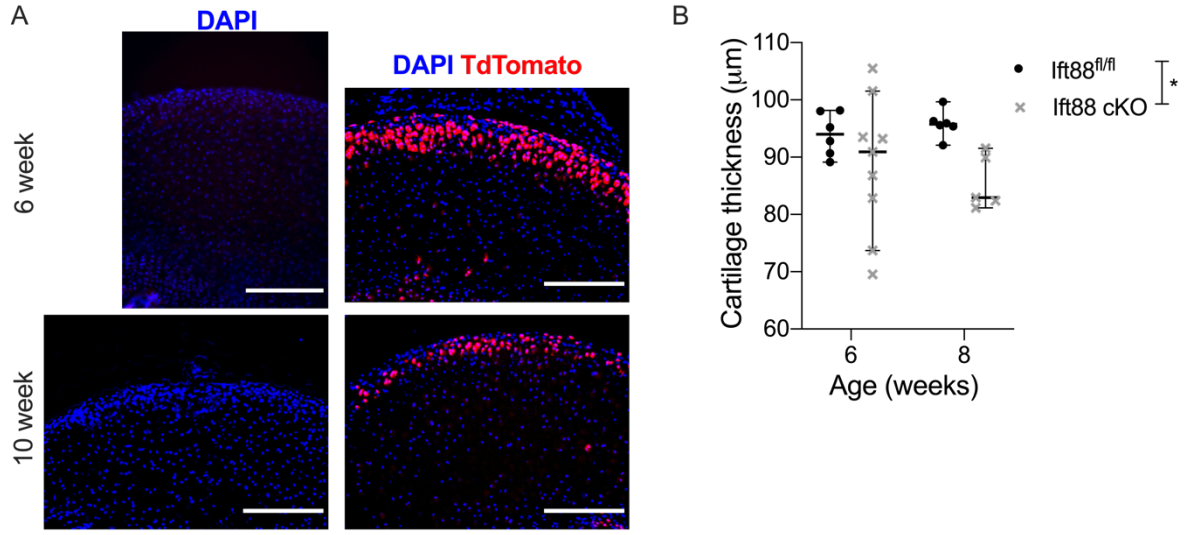

S1. A, TdTomato activated by Cre recombination in 6 and 10-week old hip articular cartilage, (scale bar= 200 µm). **B,** Average cartilage thickness of *Ift88$^{fl/fl}$* and *AggrecanCreER^{T2};Ift88$^{fl/fl}$* animals (*p<0.05). Points represent median +/- 95% confidence intervals. Analysed by two-way ANOVA, *p<0.05.

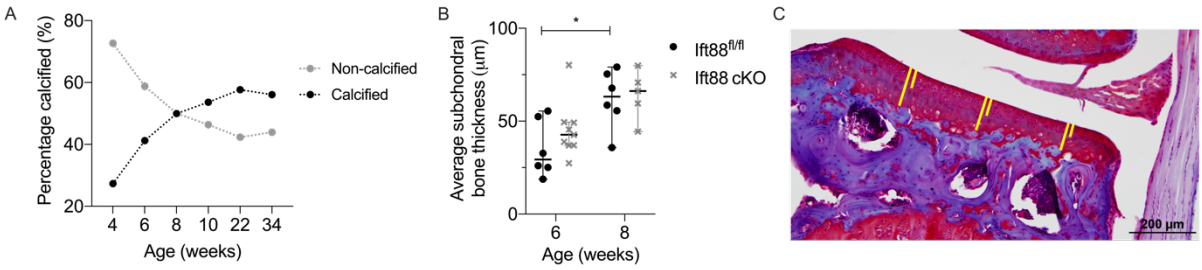

S2. A, Percentage ratios of calcified and uncalcified articular cartilage with age. **B,** Average subchondral bone thickness in 6 and 8-week old joints. **C,** Yellow lines depict measurements taken from the total thickness of the articular cartilage and the non-calcified region demarcated by the tidemark at three points across each of the medial and lateral plateaus and averaged over three consecutive sections from the middle of the joint. Minimum n= 5 in any group, apart from at 4 weeks (A) where n= 3. Points represent median +/- 95% confidence intervals. Analysed by two-way ANOVA, *p<0.05.

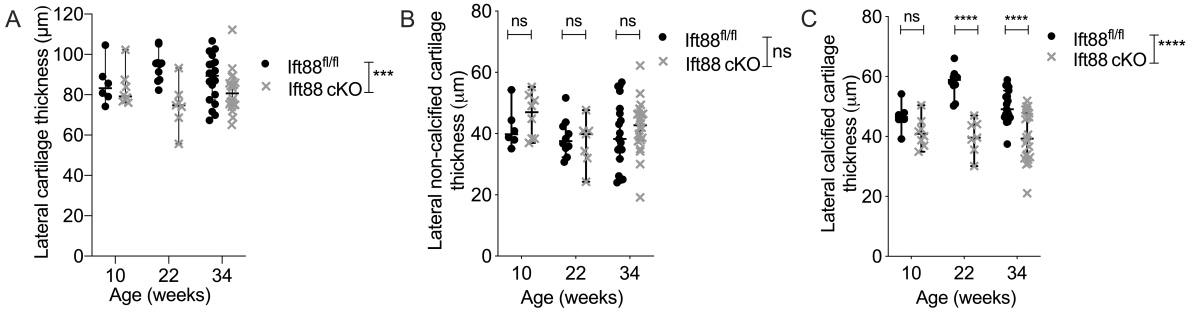

S3. A, Lateral cartilage thickness 10, 22 and 34 weeks of age. **B,** Non-calcified lateral cartilage measurements at 10, 22 and 34 weeks of age. **C,** Calcified lateral cartilage measurements 10, 22 and 34 weeks of age. Points represent median +/- 95% confidence intervals. Analysed by two-way ANOVA, ***p<0.001, ****p<0.0001.

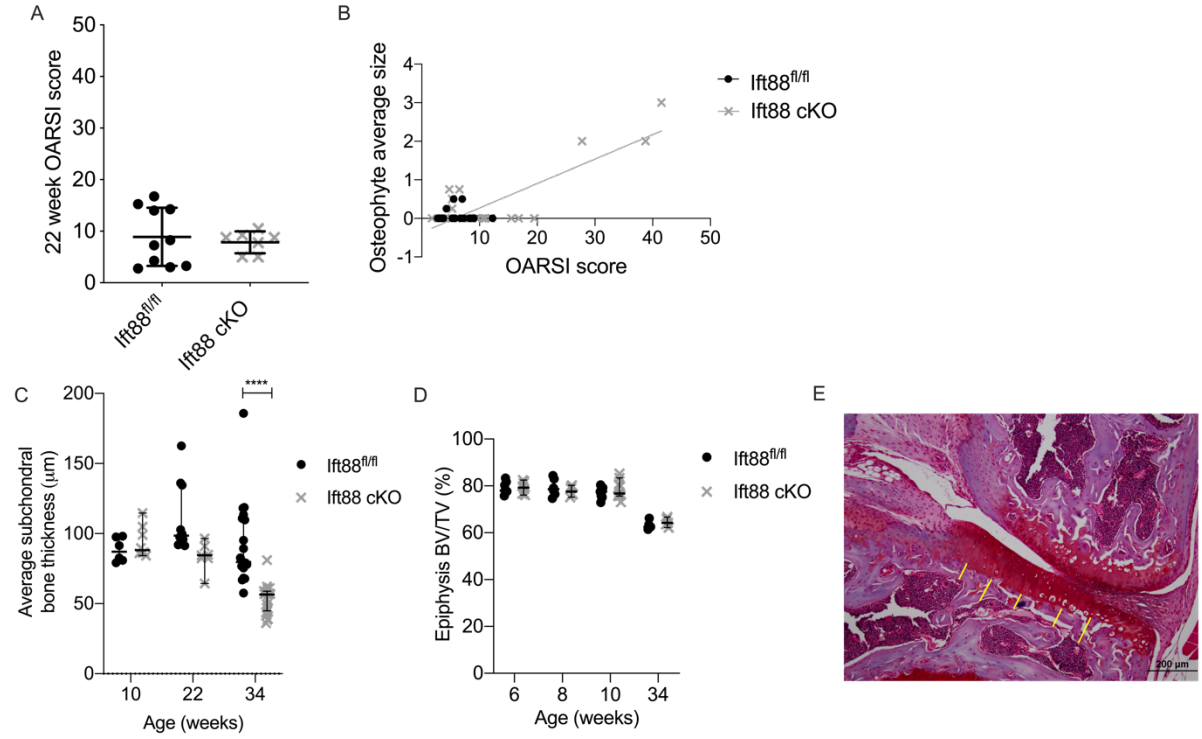

S4. A, Summed cartilage OARSI scores in sections from 22-week old animals. **B,** Osteophyte average size (data from Fig 4D) correlated with OARSI score in *Ift88*$^{fl/fl}$ and *AggrecanCreER*^{T2}*;Ift88*$^{fl/fl}$ animals using simple linear regression. **C,** Median (average) subchondral bone thickness. **D,** Bone Volume/Total Volume (BV/TV) of epiphysis in *Ift88*$^{fl/fl}$ and *AggrecanCreER*^{T2}*;Ift88*$^{fl/fl}$ animals between 6 and 34 weeks of age. **E,** Five subchondral bone measurements are taken across the plateau from the chondro-osseous junction to the top of the bone marrow and averaged across three sections from the middle of the joint. Points represent median +/- 95% confidence intervals. Analysed by two-way ANOVA, ****p<0.0001.

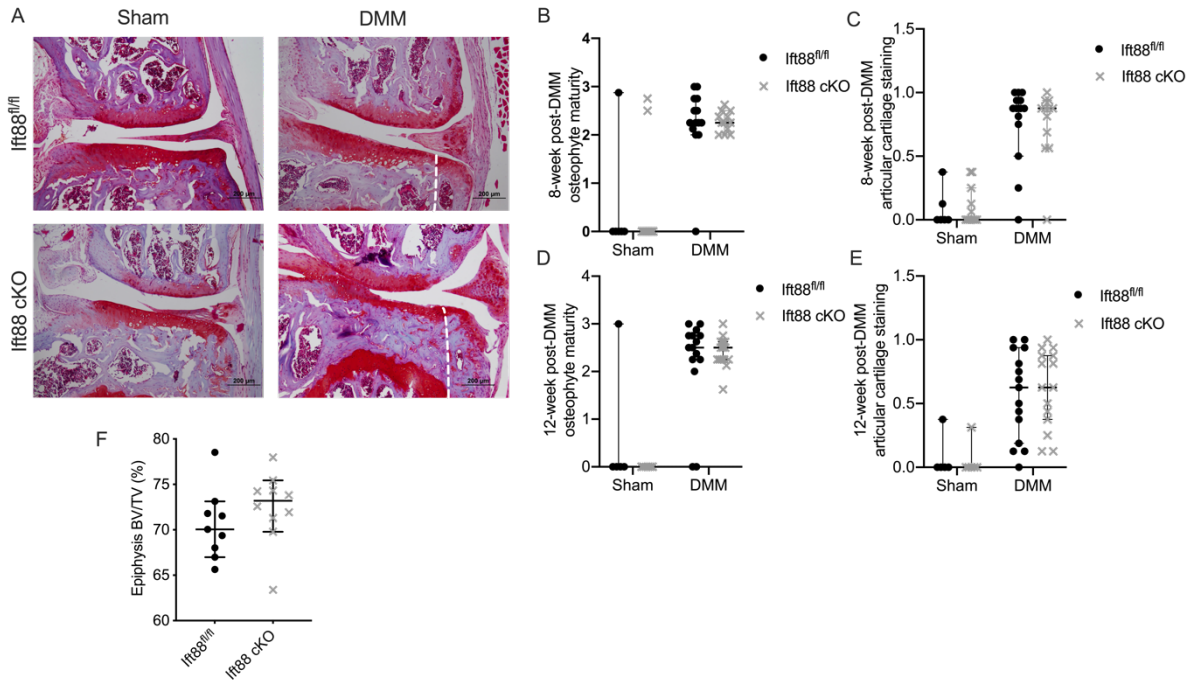

S5. A, Safranin O stained histological sections of medial compartments from Sham and DMM animals operated animals 12-weeks post-DMM surgery, (scale bar= 200 µm). **B,** Osteophyte maturity score 8-weeks post-DMM. **C,** Articular cartilage staining score 8-weeks post-DMM. **D,** Osteophyte maturity score 12-weeks post-DMM. **E,** Articular cartilage staining score 12-weeks post-DMM. **F,** Bone volume/Total volume (BV/TV) of the epiphysis 12-weeks post-DMM in *Ift88*$^{fl/fl}$ and *AggrecanCreER*^{T2}*;Ift88*$^{fl/fl}$ animals. 8-weeks post-DMM; *Ift88*$^{fl/fl}$ n= 14, *AggrecanCreER*^{T2}*;Ift88*$^{fl/fl}$ n=12. 12-weeks post-DMM; *Ift88*$^{fl/fl}$ n= 15, *AggrecanCreER*^{T2}*;Ift88*$^{fl/fl}$ = 15. Points represent median +/- 95% confidence intervals. Analysed by two-way ANOVA.

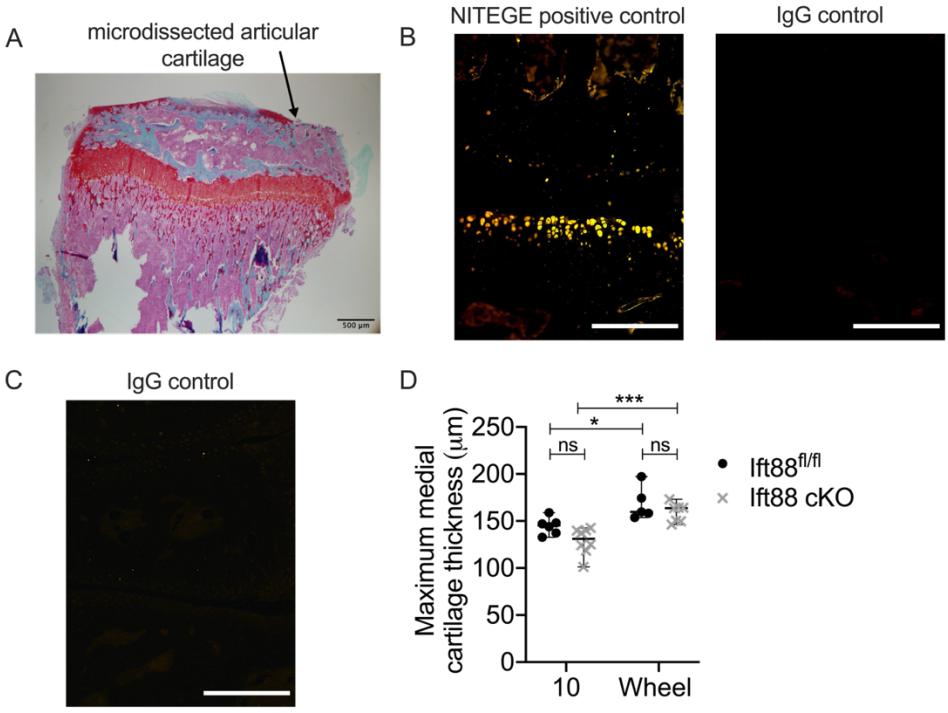

S6. A, Saf O staining of knee following micro-dissection of articular cartilage, (scale bar= 500µm). **B,** Medial compartment from animal 12-weeks post-DMM surgery was used to validate the NITEGE antibody (NITEGE positive control), and compared with IgG polyclonal. Scale bar = 200µm **C,** Control IgG section for ColX staining from 10-week old animals. Scale bar = 200µm **D,** Maximum cartilage thickness from naïve animals and mice that had access to wheel exercise (*Ift88*$^{fl/fl}$ n= 5, *AggrecanCreER*^{T2}*;Ift88*$^{fl/fl}$ n=7). Points represent median +/- 95% confidence intervals. Analysed by two-way ANOVA, *p<0.05, ***p<0.001.

Supplementary Table 1: Average housekeepers of GAPDH and HPRT

Gene	r2	Confidence intervals	p value	Corrected p value. Significance denoted at p<0.05
Tcf7l2	**0.8811**	**0.6305 to 1.361**	**0.0006**	**0.0264**
CTGF	0.8202	0.6816 to 1.879	0.002	0.088
Gli2	0.7795	0.3776 to 1.234	0.0037	0.1628
Enpp1	0.7058	0.1817 to 0.8419	0.009	0.396
Tgfbr3	0.6893	0.2059 to 1.045	0.0107	0.4708
Acan	0.6744	0.3085 to 1.708	0.0124	0.5456
Timp3	0.6286	0.1570 to 1.195	0.0189	0.8316
Wnt3a	0.9963	-0.03835 to -0.004853	0.0388	1.00
BMP2	0.5046	0.007192 to 1.398	0.0483	1.00
Ttbk2	0.4192	-0.09632 to 1.192	0.0826	1.00
Grem1	0.3598	-0.3167 to 2.221	0.116	1.00
Gli3	0.3589	-0.1728 to 1.204	0.1166	1.00
Ptch1	0.3501	-0.07868 to 0.5146	0.1223	1.00
Lrp1	0.3458	-0.1769 to 1.123	0.1252	1.00
Adamts5	0.3329	-0.3339 to 1.947	0.1343	1.00
Gli1	0.2774	-0.2958 to 1.262	0.1799	1.00
Pkd2	0.2223	-0.3095 to 1.023	0.2382	1.00
Pkd1	0.2147	-0.3276 to 1.047	0.2475	1.00
ColX	0.2053	-3.371 to 1.097	0.2596	1.00
Piezo2	0.1605	-0.7959 to 2.035	0.3254	1.00
Trpv4	0.1574	-0.6226 to 1.572	0.3305	1.00
Ngf	0.1563	-0.7367 to 1.852	0.3324	1.00
Pthr1	0.144	-0.8484 to 0.3544	0.3538	1.00
Col3	0.1354	-3.395 to 1.469	0.3698	1.00
Hhip	0.1285	-0.7538 to 1.695	0.3833	1.00
Runx2	0.1273	-0.2024 to 0.4530	0.3856	1.00
Adamts4	0.1409	-2.864 to 1.372	0.4067	1.00
Alp1	0.1147	-0.5557 to 1.182	0.4118	1.00
Mmp13	0.09278	-2.630 to 1.355	0.4632	1.00
Mmp3	0.08374	-1.770 to 0.9475	0.4869	1.00
Socs1	0.07128	-1.405 to 2.483	0.5227	1.00
Socs3	0.07027	-1.480 to 0.8413	0.5257	1.00
Inhba	0.06236	-1.063 to 1.802	0.5509	1.00
Ntrk-1	0.1433	-20.36 to 26.68	0.6215	1.00
Piezo1	0.03725	-0.8835 to 1.317	0.647	1.00
Axin2	0.03316	-0.7247 to 1.055	0.666	1.00
Cyr61	0.01988	-1.652 to 2.201	0.7391	1.00
Fgfr3	0.01723	-1.650 to 2.155	0.7567	1.00
Wnt5a	0.01745	-0.1414 to 0.1120	0.7777	1.00
Col2	0.01067	-2.461 to 3.032	0.8077	1.00
Sox9	0.00213	-1.085 to 0.9891	0.9136	1.00
BMP4	0.00208	-1.578 to 1.729	0.9146	1.00
Sp7	0.0004156	-1.110 to 1.066	0.9618	1.00
Spp1	0.00002633	-0.8598 to 0.8687	0.9904	1.00